Parkinsonism and Related Disorders 91 (2021) 59–65

Contents lists available at ScienceDirect

Parkinsonism and Related Disorders

journal homepage: www.elsevier.com/locate/parkreldis

Toll-like receptor 4 deficiency facilitates α-synuclein propagation and neurodegeneration in a mouse model of prodromal Parkinson's disease

Serena Venezia [a], Walter A. Kaufmann [b], Gregor K. Wenning [a], Nadia Stefanova [a,*]

[a] Laboratory for Translational Neurodegeneration Research, Division of Neurobiology, Department of Neurology, Medical University of Innsbruck, Austria
[b] Institute of Science and Technology Austria, Klosterneuburg, Austria

ARTICLE INFO

Keywords:
Synuclein
TLR4
Parkinson's disease
Disease progression
Microglia
DAT
CD68

ABSTRACT

The evidence linking innate immunity mechanisms and neurodegenerative diseases is growing, but the specific mechanisms are incompletely understood. Experimental data suggest that microglial TLR4 mediates the uptake and clearance of α-synuclein also termed synucleinophagy. The accumulation of misfolded α-synuclein throughout the brain is central to Parkinson's disease (PD). The distribution and progression of the pathology is often attributed to the propagation of α-synuclein. Here, we apply a classical α-synuclein propagation model of prodromal PD in wild type and TLR4 deficient mice to study the role of TLR4 in the progression of the disease. Our data suggest that TLR4 deficiency facilitates the α-synuclein seed spreading associated with reduced lysosomal activity of microglia. Three months after seed inoculation, more pronounced proteinase K-resistant α-synuclein inclusion pathology is observed in mice with TLR4 deficiency. The facilitated propagation of α-synuclein is associated with early loss of dopamine transporter (DAT) signal in the striatum and loss of dopaminergic neurons in substantia nigra pars compacta of TLR4 deficient mice. These new results support TLR4 signaling as a putative target for disease modification to slow the progression of PD and related disorders.

1. Introduction

Toll-like receptor 4 (TLR4) is a member of a family of highly conserved molecules that recognize pathogen-associated molecular patterns, including exogenous and endogenous ligands, and modulate the innate immunity response. TLR4 is found on microglia and astroglia. Multiple studies have indicated the involvement of TLR4 in the innate immune response to pathological α-synuclein [1]. In patients with Parkinson's disease (PD), dementia with Lewy bodies (DLB, and multiple system atrophy (MSA), increased mRNA and protein expression of TLR4 in the brain has been reported [2–4]. TLR4 gene polymorphism has been found in PD [5]. Experimental studies have further addressed the role of TLR4 in α-synucleinopathies. Data from our lab suggest that TLR4 on microglia mediates uptake and clearance of α-synuclein both *in vitro* and *in vivo* [6,7]. On the other hand, TLR4 signaling was implicated in the proinflammatory response of microglia in toxin models of PD [8–10] as well as in *in vitro* exposure of microglial cells to α-synuclein [7,11]. These controversial sides of TLR4 action led to the question whether this innate immunity receptor is detrimental in α-synucleinopathy and whether it may serve as a target for disease modification. In a double transgenic mouse model deficient for TLR4 and overexpressing human α-synuclein in oligodendrocytes, the neurodegeneration of substantia nigra pars compacta and the motor deficits were aggravated linked to a significant accumulation of α-synuclein in the brain [6]. Therefore, the experiment supported the beneficial role of functional TLR4 for neuronal rescue through the clearance of pathological α-synuclein. This finding was further corroborated in mice with oligodendroglial overexpression of human α-synuclein treated with monophosphoryl lipid A, a non-toxic TLR4 agonist, which showed motor improvement, rescue of nigral and striatal neurons and region-specific reduction of the density of oligodendroglial α-synuclein cytoplasmic inclusions in the absence of a marked systemic inflammatory response [12].

In light of the current understanding of seeding and spreading of the α-synuclein pathology in PD and the establishment of excellent *in vivo* propagation models [13], we sought to explore the effect of TLR4 on α-synuclein propagation and early disease progression in the mouse brain.

* Corresponding author.
E-mail address: nadia.stefanova@i-med.ac.at (N. Stefanova).

https://doi.org/10.1016/j.parkreldis.2021.09.007
Received 21 June 2021; Received in revised form 27 August 2021; Accepted 8 September 2021
Available online 11 September 2021

2. Methods

2.1. Animals and surgery

We purchased C57BL/10ScNJ mice at Jackson Laboratories (stock No.003752), bred and housed them at the Animal Facility of the Medical University of Innsbruck under a 12-h light/dark cycle with food and water available ad libitum. This mouse strain has a deletion of the TLR4 gene, so that the animals fail to express TLR4 mRNA and protein (further indicated as "TLR4-" mice [14]). Wild type mice with the same background, positive for TLR4 mRNA served as controls (further indicated as "TLR4+" mice). We genotyped the mice using the following primers: fwd: 5′- GAG ATG AAT ACC TCC TTA GTG TTG G -3‘ (m TLR4 1); rev: 5′- ATT CAA AGA TAC ACC AAC GGC TCT GA -3′(m TLR4 2); fwd: 5′- CTC AGG GTC GAC TGC CTT AG -3‘ (m a-syn1), rev: 5′- TGC ACT CGA AGA GTC CCT TT -3′(m a-syn 2), resulting in a band of 415 bp for mTLR4 and a band of 760 bp for mα-Syn. All experiments were performed according to the Austrian and European law and with permission by the Federal Ministry for Science, Research and Economy of Austria, BMWFW-66.011/0122-WF/V/3b/2014. All efforts were made to minimize the number of animals used and their suffering.

For stereotaxic surgery, ten TLR4- and ten TLR4+ mice matched in sex, at 12 weeks of age, received deep isoflurane inhalation anesthesia. The skull was fenestrated and two stereotaxic unilateral striatal deposits of 3 μg human α-synuclein preformed fibrils (hu-αS PFFs) were inoculated with a 5 μl Hamilton syringe: one of 2 μl with coordinates AP: 0.5 mm; L: 1.8 mm; V: −3.5 mm, and one of 1 μl with coordinates AP: −0.5 mm; L: 1.8 mm; V: −2.5 mm. The tooth bar was set at 0. Half of the mice per group were sacrificed 30 days after the surgery and the second half – 90 days after the surgery for further histological analysis.

2.2. Preparation and characterization of PFFs of recombinant full-length hu-αS

The purification and endotoxin removal of the recombinant full-length hu-αS were done as previously described [7]. The assembly of the protein was achieved following the standardized protocol of Volpicelli-Daley et al. [15]. To control for amyloid fibril formation, 10 μl samples were added to 1 mL 20 μM ThT (SigmaAldrich) in PBS and fluorescence emission spectra were immediately recorded at 465–600 nm with excitation at 440 nm. Aliquots with a concentration of 2 mg/mL were kept at −80 °C and thawed immediately before inoculation.

2.3. Electron microscopy, negative staining of hu-αS PFFs

Samples were kept at −80 °C and thawed to 4 °C just before the staining. Carbon-coated 300 mesh copper grids (Electron Microscopy Sciences, CF300-CU) were plasma cleaned for 2 min at pressure 7x10-1 mbar in an ELMOTM glow discharge unit (Agar Scientific Ltd. UK). 5 μl of sample solution was loaded onto a grid, and proteins allowed to adhere for 5 min at RT. Excess of solution was removed with filter paper and samples washed briefly in a drop of chilled distilled water. Samples were stained with 5 μl of 2% aqueous uranyl-acetate (w/v; AL-Labortechnik e.U. Amstetten, 77870.02) for 1 min at RT. Excess solution was removed with filter paper and grids air-dried. Samples were observed under a Tecnai 10 transmission electron microscope (Thermo Fisher Scientific GmbH) operated at 80 kV, and equipped with a side-mounted camera OSIS MegaView G3 (Electron Microscopy Soft Imaging Solutions [EMSIS] GmbH; Muenster, Germany). Radius software (EMSIS) was used for image processing and dissection. GraphPad Prism 8 was used for data analysis and processing.

Sampling and analysis: grid squares were chosen at random on a mesh grid and all stained filaments were analyzed within. This was repeated until the predefined statistical number of samples had been reached. In case of length distribution measurements, images were taken at low magnification to ensure visibility of both filament ends within a micrograph. In case of width measurements, images were taken at 65 kx. To determine the diameter of hu-αS oligomers, grid squares were chosen at random and images taken at 110 kx. All identifiable oligomers within were analyzed until the predefined sample number had been reached.

2.4. Immunohistochemistry

Mice were transcardially perfused with 20 mL phosphate buffered saline (PBS) for 5 min under overdose of Thiopental. The brains were removed from the skull and immersion fixed in 4% paraformaldehyde in PBS for 24h at 4 °C. The fixed brains were slowly frozen in 2-methylbutane and kept at −80 °C until further processing. The brains were cut coronally in series of sections with thickness of 40 μm using a cryotome (Leica). The series included every sixth section. The sections were immunohistochemically stained with the following primary antibodies: rabbit anti-pS129 α-synuclein (Abcam, UK), rabbit anti-mouse α-synuclein (Cell Signaling), mouse anti-ubiquitin (Chemicon), rat anti-CD68 (Serotec), rat anti-dopamine transporter (DAT, Millipore), rabbit anti-tyrosine hydroxylase (TH, Millipore), rabbit anti-p62 (Cell Signaling), rat anti-CD11b (Serotec), followed by respective secondary antibodies: biotinylated or Alexa488/594 conjugated anti-rabbit, anti-rat, or anti-mouse IgG. The immunohistochemical reaction was visualized with either ABC complex and 3,3′-diaminobenzidine or by fluorescence.

2.5. Proteinase K digestion on frozen sections

For the detection of α-synuclein aggregation, free-floating brain sections were mounted on charged glass slides and allowed to adhere overnight at 37 °C. Sections were incubated with Proteinase K (PK, Ambion) at a final concentration of 2 mg/mL in PBS for 10 min at room temperature. Sections were washed 3 × 5 min with PBS and then blocked with 10% goat serum followed by overnight incubation with rabbit anti-pS129 α-synuclein (Abcam, UK) at 4 °C, 3 × 5min wash in PBS and 40min incubation in Alexa488 conjugated anti-rabbit IgG (Thermo Fischer Scientific). The sections were coverslipped with fluoromount.

2.6. Image analysis

Series of pS129 and CD68 immunostained sections per mouse (240 μm intervals between sections in each series) were analyzed on blind coded slides. A rating scale of pS129 aggregate pathology as previously described [16,17] was applied: absent (−), sparce (+), mild (++), moderate (+++), severe (++++) to estimate the propagation and severity of the pathology ipsilaterally and contralaterally to the PFF inoculation. Similarly, CD68-positive microglia was assessed throughout the brain of each mouse and rated per region as absent (0), mild (1), moderate (2), intense (3).

DAT immunofluorescent signal in the striatum was estimated by ImageJ. Photos of the ipsilateral and contralateral striatum at Bregma 0.26 mm on blind coded slides were taken with constant camera settings on Leica DMi8 Microscope provided with a digital camera and a Leica Imaging Software (LAS). The striatum was delineated and the relative intensity of the signal was measured. The background signal was measured in the corpus callosum and the relative intensity of DAT immunostaining was corrected for each image. A mean value per striatum was generated as the average of the values in the three sections analyzed per animal.

TH-immunostained sections throughout the SNc on blind-coded slides were used to count the number of TH-positive neurons in the ipsi- and contralateral to the PFFs injection side with the aid of a Nikon E−800 microscope equipped with Nikon digital camera DXM1200 and the StereoInvestigator software (Microbrightfield Europe e.K). In each section, the area of the SNc was delineated and a stereological analysis with a counting frame 50μm/50 μm, a grid of 100μm/200 μm and periodicity of 6 was applied.

2.7. Statistical analysis

SPSS27 and Graph Pad Prism 8 were used for data analysis and graphic representation. In each experimental group and each time-point after surgery, three mice were used for the statistical analysis. For parametric data, comparisons were performed with two-way ANOVA with the factors "genotype" and "brain region" followed by correction for multiple comparisons with the Sidak's posthoc test. For the non-parametric data sets, we performed multiple pairwise comparisons of group distributions by Friedman's two-way ANOVA by ranks as well as Kruskal-Wallis H test for multiple comparisons.

3. Results

3.1. Distribution of CD68-positive microglia after hu-αS PFF inoculation

We showed previously that TLR4 deficiency interferes with the clearance of extracellular α-synuclein by microglia [6,7]. CD68 is a lysosomal marker of macrophages/microglia and we here sought to identify whether TLR4 deficiency may result in changes in the expression of CD68-positive microglia after inoculation of hu-αS PFFs. Indeed, the injection of hu-αS PFFs (Fig. 1) in the brain of TLR4+ and TLR4- mice triggered early ipsilateral CD68 microglial activation especially strong along the inoculation tract in the striatum and cortex, but also in the SNc and BLA in TLR4+ mice already at 30 days post injection (Fig. 2A and B). Interestingly, the CD68-positive activation of microglia reached significantly higher levels in the SNc of TLR4+ mice, suggesting increased microglial lysosomal reactivity, triggered by the propagating extracellular seeds of α-synuclein as compared to the one in TLR4- mice (Fig. 2B). In the contralateral hemisphere, mild increase of the CD68 signal was identified in TLR4+ mice, but not in TLR4- mice, however the differences were not statistically significant (Fig. 2B). At 90 days post inoculation, the CD68 response in both the ipsilateral and contralateral hemisphere was significantly higher in TLR4+ vs TLR4- mice when distributions were compared with the non-parametric Friedman's 2-way ANOVA by ranks. However, the differences in the single analyzed regions lost significance after a multiple comparison with the Kruskal-Wallis test (Fig. 2C and D). The overall reduced CD68 labeling in TLR4- brains 90 days after the hu-αS PFFs inoculation was accompanied by reduced expression of p62 expression in microglia (Fig. 2D).

3.2. Propagation of α-synuclein pathology

Thirty days after inoculation of hu-αS PFFs, we found few single pS129-positive profiles along the inoculation tract in the ipsilateral striatum of both TLR4- and TLR4+ mice. We identified pS129-positive profiles also in the cortex, corpus callosum, and the basolateral amygdala in TLR4- mice, but not in TLR4+ mice (Fig. 3A,C). In neither of the two genotypes, there was any detectable pS129-immunoreactivity in the contralateral hemisphere at this stage. However, 90 days after hu-αS PFF inoculation both TLR4+ and TLR4- mice showed propagation of the α-synuclein pathology (Fig. 3A–C). We identified numerous pS129-positive cytoplasmic inclusions in the ipsilateral striatum and in anatomically connected regions including cortex (prelimbic, cingulate, sensory, motor, insular), basolateral amygdala (Fig. 3B), substantia nigra, ventral tegmental area, and dorsal raphe nucleus. pS129-positive

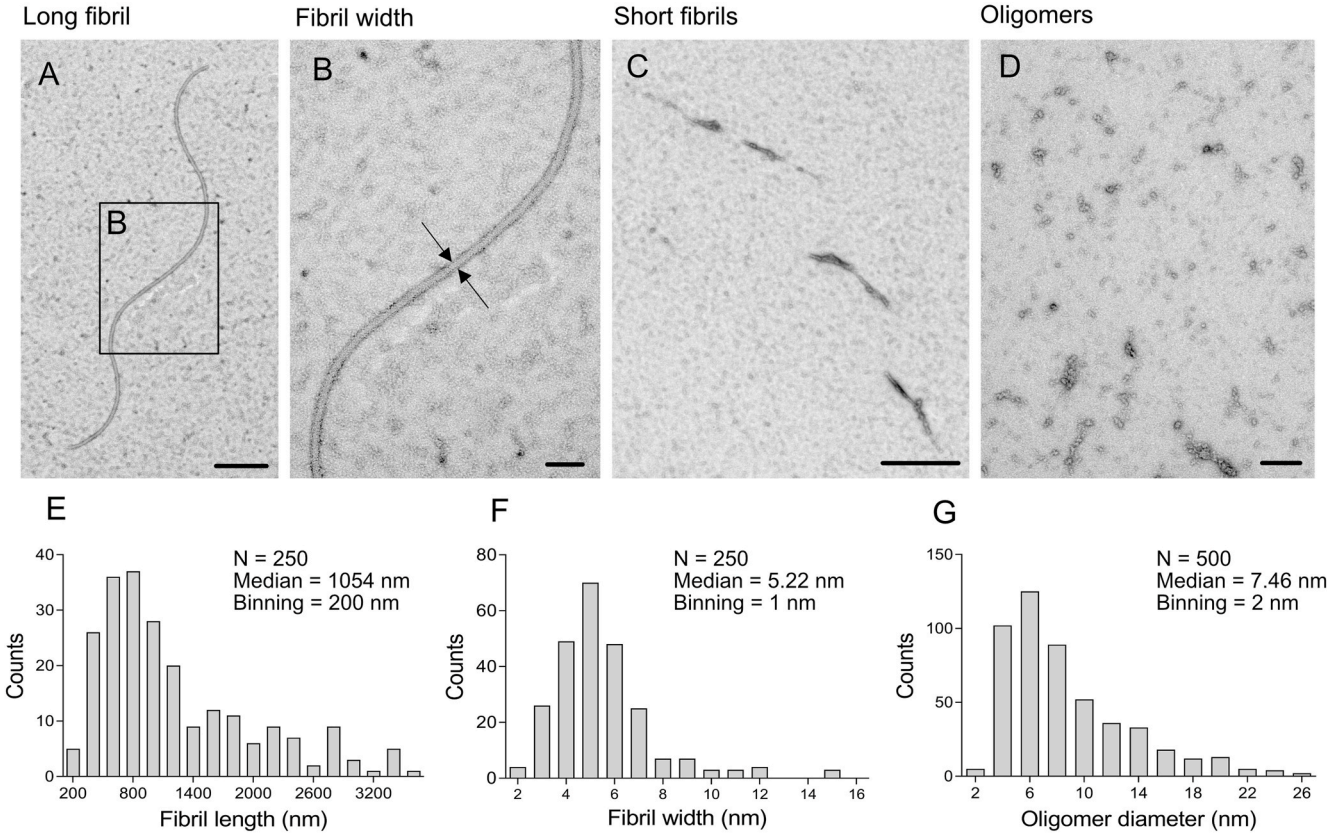

Fig. 1. Characterization of hu-αS PFF preparation - negative staining and transmission electron microscopy. (A–D) TEM micrographs of negatively stained hu-αS PFFs. (A) Low magnification image of a characteristic long fibril. Scale bar, 200 nm. (B) Fibril width at higher magnification with black arrows indicating the placement of the measuring points. Scale bar, 50 nm. (C) Individual short fibrils. Scale bar, 500 nm. (D) hu-αS oligomers. Scale bar, 100 nm. (E–G) Scatter plots representing the frequency distributions of fibril length (E), fibril width (F) and oligomer diameter (G) for evaluated numbers of samples. We observed hu-αS fibrils of variable sizes with an average length of 1.054 μm (min = 0.175 μm, max = 9.604 μm) and average width of 5.22 nm (min = 2.36 nm, max = 17.89 nm), as well as hu-αS oligomers with an average diameter of 7.46 nm (min = 2.02 nm, max = 33.48 nm), and half of them ranging between 5.2 and 11.2 nm.

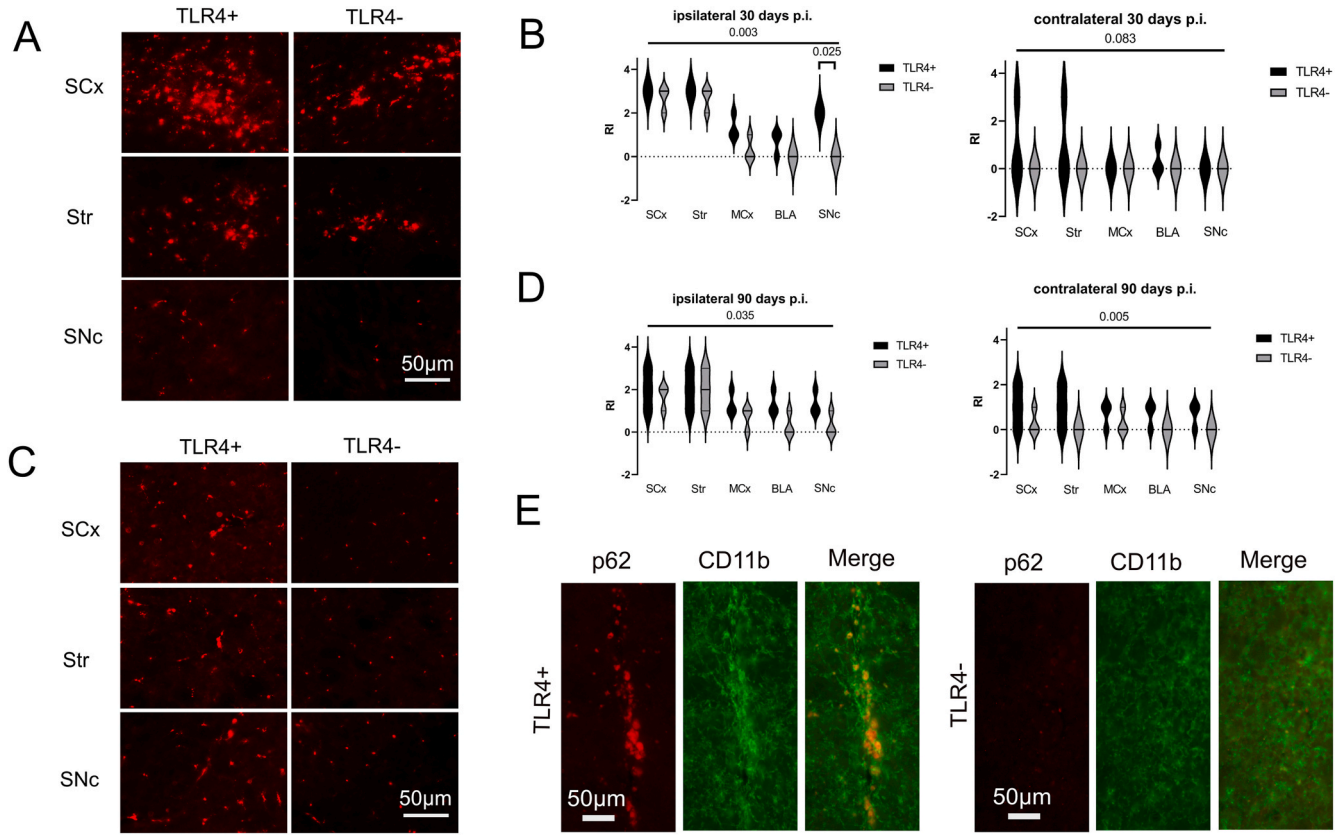

Fig. 2. CD68-positive microglia in the brains of mice receiving hu-αS PFFs striatal inoculation. (A) Representative images of immunofluorescence for CD68 in wild type (TLR+) and TLR4-deficient (TLR4-) mice 30 days after the hu-αS PFFs striatal inoculation, ipsilaterally. **(B)** Violin plots with a comparison of the distribution of the CD68-positive signal in TLR4+ and TLR4- mice 30 days after the hu-αS PFFs striatal inoculation; non-parametric Friedman's two-way ANOVA by rank and Kruskal-Wallis multiple comparisons test. **(C)** Representative images of immunofluorescence for CD68 in wild type (TLR+) and TLR4-deficient (TLR4-) mice 90 days after the hu-αS PFFs striatal inoculation, contralaterally **(D)** Comparison of the intensity of CD68-positive signal in TLR4+ and TLR4- mice 90 days after the hu-αS PFFs striatal inoculation; non-parametric Friedman's two-way ANOVA by rank and Kruskal-Wallis multiple comparisons test. Abbreviations: STR, striatum; SCx, sensory cortex; MCx, motor cortex; BLA, basolateral amygdala; SNc, substantia nigra pars compacta; p. i., post inoculation. (E) Double immunofluorescence for p62 (red) and CD11b (green) in TLR+ and TLR4- brains, 90 days after hu-αS PFFs striatal inoculation. (For interpretation of the references to colour in this figure legend, the reader is referred to the Web version of this article.)

cytoplasmic inclusions were identified also in white matter tracts including the corpus callosum, capsula externa, capsula interna, and the medial forebrain bundle. In the contralateral side, pS129-positive cytoplasmic inclusions were identified in the striatum, cortex and basolateral amygdala of TLR4- mice but not in TLR4+ mice (Fig. 3A–C). The quantification of the α-synuclein pathology demonstrated significantly higher density in TLR4 deficient mice 90 days after α-synuclein inoculation (Fig. 3C). The cytoplasmic inclusion pathology was exclusively positive for endogenous mouse α-synuclein but not for the inoculated human α-synuclein and the intracellular accumulation of mouse α-synuclein co-localized with ubiquitin (Fig. 3D). PK digestion of midbrain sections demonstrated PK resistance of the pS129-positive cytoplasmic inclusions in both TLR4+ and TLR4- brains (Fig. 3E).

3.3. Signs of nigral degeneration and dysregulated striatal dopamine transmission after hu-αS PFFs striatal inoculation

DAT is a useful and sensitive probe for nigrostriatal dopaminergic integrity associated with the disease progression in PD [18]. We here estimated the ROD of the striatal DAT signal in TLR4+ and TLR4- mice 90 days after receiving inoculation of hu-αS PFFs. We identified significant reduction of the DAT signal in the ipsilateral striatum in TLR4 deficient mice, 20% lower as compared to the one in TLR4+ mice (Fig. 4A and B). At this stage, no significant difference in the DAT density was found between the ipsi- and contralateral to the inoculation striatum (Fig. 4B). The assessment of the number of dopaminergic neurons in the SNc showed significant loss in TLR4-, but not in TLR4+ ipsilateral SNc (Fig. 4E and F).

4. Discussion

We provide novel evidence of TLR4 role in the progression of PD-like neurodegeneration. Our data demonstrate that TLR4 deficiency in mice is associated with a deficit in the autophago-lysosomal activity (CD68 and p62) of microglial cells in response to hu-αS PFFs and a following facilitation of the propagation of the inclusion pathology consisting of PK-resistant α-synuclein cytoplasmic aggregates. Finally, the inoculation of hu-αS PFFs in TLR4-deficient mice results in deficits of the dopaminergic innervation of the striatum and significant loss of dopaminergic neurons in SNc 90 days after inoculation at a time when the dopaminergic system of TLR4+ mice is not yet affected by the degenerative process. Linking the current data to previous observations [6,7], we conclude that the reduced clearance of extraneuronal α-synuclein seeds by TLR4-deficient microglia may play a significant role in the propagation of α-synuclein aggregates and thereafter in the progression of PD and other α-synucleinopathies.

In the current study, we applied a well-established PD model of *in vivo* α-synuclein seed inoculation followed by Lewy pathology propagation [13,19]. The ultrastructural characterization of the applied hu-αS PFFs demonstrated size distributions of the oligomers and filaments similar to those reported previously [20,21]. Earlier studies have identified reduced seeding activity of human α-synuclein PFFs as compared

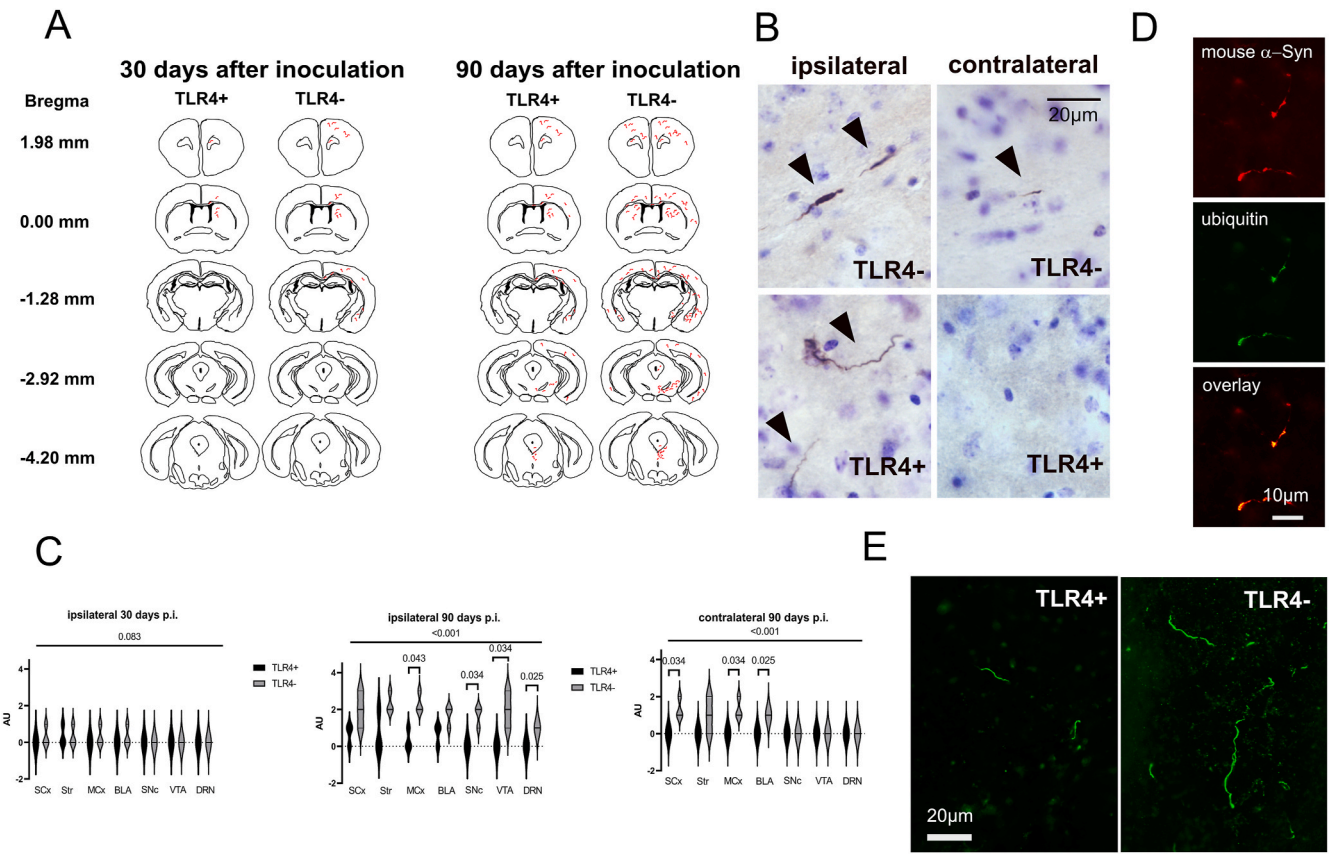

Fig. 3. Spreading of cytoplasmic inclusion pathology after hu-αS PFFs inoculation in the mouse striatum. (A) α-synuclein pathology spreading pattern in wild type (TLR+) and TLR4-deficient (TLR4-) mice. **(B)** Representative images of pS129 immunohistochemical identification of pS129-positive neurites (arrows) ipsilaterally and contralaterally to the hu-αS PFFs inoculation side in the basolateral amygdala. **(C)** Violin plots with a comparison of the distribution of α-synuclein pathology in TLR+ and TLR4- mice; non-parametric Friedman's two-way ANOVA by rank and Kruskal-Wallis multiple comparisons test. **(D)** Double immunofluorescence for mouse α-synuclein and ubiquitin. (E) PK resistant pS129 cytoplasmic inclusions in the SNc of TLR4+ and TLR4- mice 90 days after the hu-αS PFFs striatal inoculation. Abbreviations: STR, striatum; SCx, sensory cortex; MCx, motor cortex; BLA, basolateral amygdala; SNc, substantia nigra pars compacta; VTA, ventral tegmental area; DRN, dorsal raphe nucleus; p. i., post inoculation.

to mouse α-synuclein PFFs in the wild type rodent brain [22,23]. In accordance with these observations, in our experiment in wild type mice, up to 3 months after the inoculation of hu-αS PFFs, we detected only mild α-synuclein cytoplasmic inclusion pathology in anatomically associated brain areas. In this experimental model, TLR4 deficiency facilitated the propagation of the α-synuclein pathology within three months after inoculation of the hu-αS PFFs. We provide evidence that the intracellular aggregates of phosphorylated α-synuclein pS129, although triggered by hu-αS PFFs, are composed predominantly of ubiquitinated endogenous mouse α-synuclein corroborating previous reports [15]. Importantly, in both TLR4+ and TLR4- mice receiving hu-αS PFFs, the inclusion pathology consisted of PK-resistant α-synuclein aggregates.

The neuronal spreading of the aggregate pathology in anatomically defined circuits supports the *trans*-synaptic spreading of the α-synuclein pathology, which seems to be a leading mechanism in the propagation models of α-synucleinopathies [24]. This specific mechanism of spreading of α-synuclein pathology may not be directly affected by TLR4. Therefore, the *trans*-synaptic propagation of α-synuclein pathology may be a reason for a certain masking of the differences between TLR4+ and TLR4- mice as observed in our study. However, other molecular mechanisms involved in the cell-to-cell protein spreading like exocytosis/transmembrane relocation of the protein are responsible for the additional extracellular spreading of α-synuclein seeds [25]. Changes in the microglial activity may interfere with the TLR4-dependent synucleinophagy and clearance of such extracellular pathological α-synuclein [6,26]. Our observations support the role of TLR4-mediated autophago-lysosomal response of microglia linked to modulation of the clearance of extracellular α-synuclein and followed by limited cell-to-cell seed spreading of the pathology. Therefore, our results add to the understanding on the fundamental role of the immune responses in the pathogenesis of α-synucleinopathies [27,28].

The finding of facilitated α-synucleinopathy propagation in TLR4-deficient mice receiving hu-αS PFFs was accompanied by a significant reduction of DAT levels in the ipsilateral striatum and significant neuronal loss in the ipsilateral SNc as compared to those in TLR4+ mice. Reduced DAT binding is a classical early imaging biomarker of PD [29]. DAT is a reliable marker of presynaptic terminals of dopamine cells in the striatum and together with the evidence of accelerated neurodegeneration in the SNc support the role of TLR4 in α-synuclein triggered pathology. Therefore, in the current propagation model we generated an early PD phenotype by a facilitation of extracellular α-synuclein seeds' spreading due to the reduced microglial clearance linked to TLR4 deficiency. One may argue that TLR4 deficit *per se* may interfere with the level of DAT or TH, however in the side contralateral to the hu-αS PFFs inoculation we detected no differences in the DAT or TH expression between TLR4+ and TLR4- mice at this stage, respectively discarding this option.

In summary, the current study extends the understanding on the role of TLR4 for the microglia-mediated clearance of pathological α-synuclein [6,7,26]. We demonstrate TLR4 impact on the propagation of the Lewy-like pathology and the progression of striatonigral neurodegeneration in a model of prodromal PD. Together with the reported association of TLR4 polymorphism and the risk of PD [5], our results

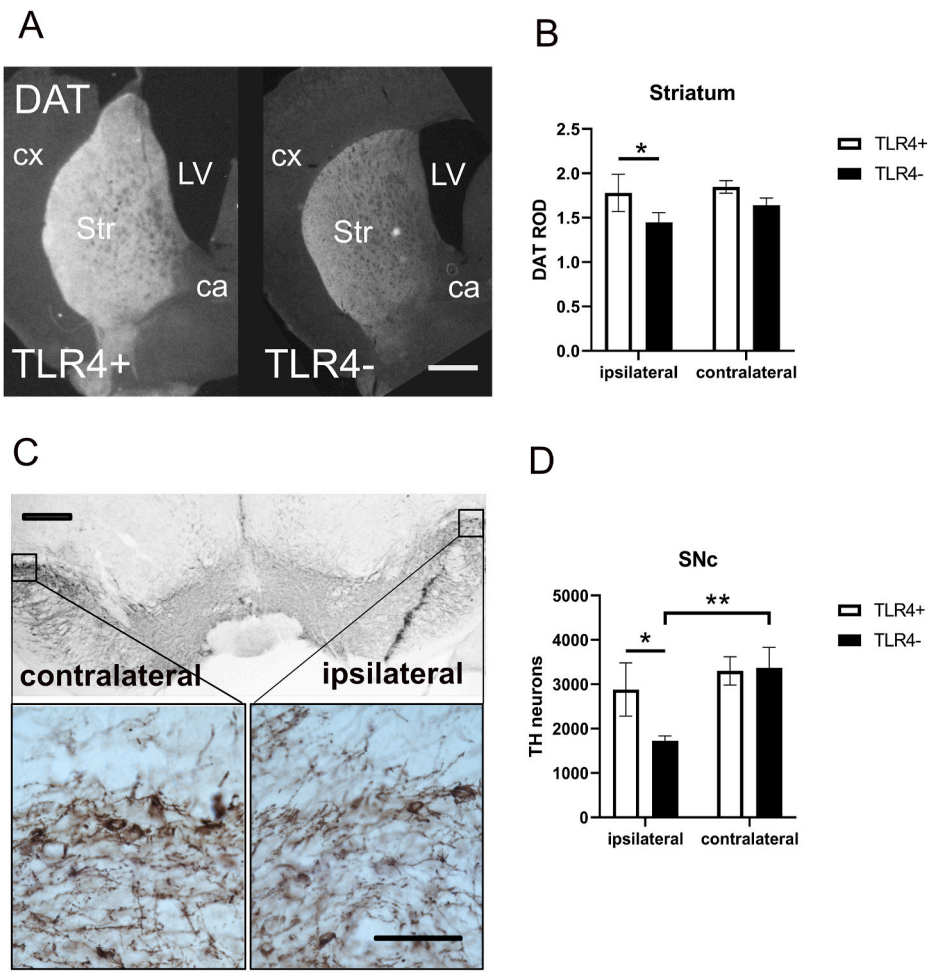

Fig. 4. Dopaminergic striatonigral degeneration after hu-αS PFFs inoculation. (A) DAT-immunofluorescence in the striatum of TLR4+ and TLR4- mice 90 days after hu-αS PFFs inoculation. Scale bar, 550 μm. Abbreviations: Str, striatum, cx, cortex; ca, anterior commissure; LV, lateral ventricle. **(B)** Comparison of the relative optical density of DAT-immunofluorescence in the striatum of TLR4+ and TLR4- mice ipsilaterally and contralaterally to the hu-αS PFFs inoculation side; two-way ANOVA with Sidak's multiple comparisons test, *$p < 0.05$. (C) TH-immunoreactivity in the SNc of a TLR4- mouse ipsilaterally and contralaterally to the hu-αS PFFs inoculation side; Scale bar, 500 μm, Scale bar of insets, 100 μm. (D) Comparison of the number of TH-immunopositive neurons in the SNc of TLR4+ and TLR4- mice ipsilaterally and contralaterally to the hu-αS PFFs inoculation side; two-way ANOVA with Sidak's multiple comparisons test, *$p < 0.05$, **$p < 0.01$.

strongly support targeting TLR4-mediated synucleinophagy as a strategy to slow the disease progression in PD and related synucleinopathies [12]. On the other hand, prolonged exposure to low levels of oligomeric α-synuclein has been suggested to lead to TLR4 sensitization resulting in a proinflammatory neurotoxic profile of astrocytes and microglia [30]. Therefore, long-term preferential targeting of the different TLR4 signaling pathways – neuroinflammatory or related to the clearance of α-synuclein - may lead to the selective modulation of the disease progression in α-synucleinopathies.

Acknowledgements

This study was supported by grants of the Austrian Science Fund (FWF) F4414 and W1206-08. Electron microscopy was performed at the Scientific Service Units (SSU) of IST-Austria through resources provided by the Electron Microscopy Facility.

References

[1] A. Kouli, C.B. Horne, C.H. Williams-Gray, Toll-like receptors and their therapeutic potential in Parkinson's disease and α-synucleinopathies, Brain Behav. Immun. 81 (2019) 41–51.
[2] M. Letiembre, Y. Liu, S. Walter, W. Hao, T. Pfander, A. Wrede, W. Schulz-Schaeffer, K. Fassbender, Screening of innate immune receptors in neurodegenerative diseases: a similar pattern, Neurobiol. Aging 30 (5) (2009) 759–768.
[3] T. Brudek, K. Winge, T.K. Agander, B. Pakkenberg, Screening of Toll-like receptors expression in multiple system atrophy brains, Neurochem. Res. 38 (6) (2013) 1252–1259.
[4] N. Stefanova, M. Reindl, M. Neumann, P.J. Kahle, W. Poewe, G.K. Wenning, Microglial activation mediates neurodegeneration related to oligodendroglial alpha-synucleinopathy: implications for multiple system atrophy, Mov. Disord. 22 (15) (2007) 2196–2203.
[5] J. Zhao, X. Han, L. Xue, K. Zhu, H. Liu, A. Xie, Association of TLR4 gene polymorphisms with sporadic Parkinson's disease in a Han Chinese population, Neurol. Sci. : official journal of the Italian Neurological Society and of the Italian Society of Clinical Neurophysiology 36 (9) (2015) 1659–1665.
[6] N. Stefanova, L. Fellner, M. Reindl, E. Masliah, W. Poewe, G.K. Wenning, Toll-like receptor 4 promotes alpha-synuclein clearance and survival of nigral dopaminergic neurons, Am. J. Pathol. 179 (2) (2011) 954–963.
[7] L. Fellner, R. Irschick, K. Schanda, M. Reindl, L. Klimaschewski, W. Poewe, G. K. Wenning, N. Stefanova, Toll-like receptor 4 is required for alpha-synuclein dependent activation of microglia and astroglia, Glia 61 (3) (2013) 349–360.
[8] C. Conte, L. Roscini, R. Sardella, G. Mariucci, S. Scorzoni, T. Beccari, L. Corte, Toll like receptor 4 affects the cerebral biochemical changes induced by MPTP treatment, Neurochem. Res. 42 (2) (2017) 493–500.
[9] G. Mariucci, R. Pagiotti, F. Galli, L. Romani, C. Conte, The potential role of toll-like receptor 4 in mediating dopaminergic cell loss and alpha-synuclein expression in the acute MPTP mouse model of Parkinson's disease, J. Mol. Neurosci. : M O 64 (4) (2018) 611–618.
[10] M. Campolo, I. Paterniti, R. Siracusa, A. Filippone, E. Esposito, S. Cuzzocrea, TLR4 absence reduces neuroinflammation and inflammasome activation in Parkinson's diseases in vivo model, Brain Behav. Immun. 76 (2019) 236–247.
[11] Q.H. Shao, W.F. Yan, Z. Zhang, K.L. Ma, S.Y. Peng, Y.L. Cao, Y.H. Yuan, N.H. Chen, Nurr1: a vital participant in the TLR4-NF-κB signal pathway stimulated by α-synuclein in BV-2 cells, Neuropharmacology 144 (2019) 388–399.
[12] S. Venezia, V. Refolo, A. Polissidis, L. Stefanis, G.K. Wenning, N. Stefanova, Toll-like receptor 4 stimulation with monophosphoryl lipid A ameliorates motor deficits and nigral neurodegeneration triggered by extraneuronal alpha-synucleinopathy, Mol. Neurodegener. 12 (1) (2017) 52.
[13] K.C. Luk, V. Kehm, J. Carroll, B. Zhang, P. O'Brien, J.Q. Trojanowski, V.M. Lee, Pathological alpha-synuclein transmission initiates Parkinson-like neurodegeneration in nontransgenic mice, Science 338 (6109) (2012) 949–953.
[14] A. Poltorak, X. He, I. Smirnova, M.Y. Liu, C. Van Huffel, X. Du, D. Birdwell, E. Alejos, M. Silva, C. Galanos, M. Freudenberg, P. Ricciardi-Castagnoli, B. Layton, B. Beutler, Defective LPS signaling in C3H/HeJ and C57BL/10ScCr mice: mutations in Tlr4 gene, Science 282 (5396) (1998) 2085–2088.
[15] L.A. Volpicelli-Daley, K.C. Luk, V.M. Lee, Addition of exogenous alpha-synuclein preformed fibrils to primary neuronal cultures to seed recruitment of endogenous

alpha-synuclein to Lewy body and Lewy neurite-like aggregates, Nat. Protoc. 9 (9) (2014) 2135–2146.
[16] K.C. Luk, V.M. Kehm, B. Zhang, P. O'Brien, J.Q. Trojanowski, V.M. Lee, Intracerebral inoculation of pathological alpha-synuclein initiates a rapidly progressive neurodegenerative alpha-synucleinopathy in mice, J. Exp. Med. (2012).
[17] N.L. Rey, S. George, J.A. Steiner, Z. Madaj, K.C. Luk, J.Q. Trojanowski, V.M. Lee, P. Brundin, Spread of aggregates after olfactory bulb injection of α-synuclein fibrils is associated with early neuronal loss and is reduced long term, Acta Neuropathol. 135 (1) (2018) 65–83.
[18] J.H. Kordower, C.W. Olanow, H.B. Dodiya, Y. Chu, T.G. Beach, C.H. Adler, G. M. Halliday, R.T. Bartus, Disease duration and the integrity of the nigrostriatal system in Parkinson's disease, Brain 136 (Pt 8) (2013) 2419–2431.
[19] L.A. Volpicelli-Daley, K.C. Luk, T.P. Patel, S.A. Tanik, D.M. Riddle, A. Stieber, D. F. Meaney, J.Q. Trojanowski, V.M. Lee, Exogenous α-synuclein fibrils induce Lewy body pathology leading to synaptic dysfunction and neuron death, Neuron 72 (1) (2011) 57–71.
[20] G.A.P. de Oliveira, J.L. Silva, Alpha-synuclein stepwise aggregation reveals features of an early onset mutation in Parkinson's disease, Communications biology 2 (2019) 374.
[21] S. Aulić, T.T. Le, F. Moda, S. Abounit, S. Corvaglia, L. Casalis, S. Gustincich, C. Zurzolo, F. Tagliavini, G. Legname, Defined α-synuclein prion-like molecular assemblies spreading in cell culture, BMC Neurosci. 15 (2014) 69.
[22] K.C. Luk, D.J. Covell, V.M. Kehm, B. Zhang, I.Y. Song, M.D. Byrne, R.M. Pitkin, S. C. Decker, J.Q. Trojanowski, V.M. Lee, Molecular and biological compatibility with host alpha-synuclein influences fibril pathogenicity, Cell Rep. 16 (12) (2016) 3373–3387.
[23] N. Van Den Berge, N. Ferreira, T.W. Mikkelsen, A.K.O. Alstrup, G. Tamgüney, P. Karlsson, A.J. Terkelsen, J.R. Nyengaard, P.H. Jensen, P. Borghammer, Ageing promotes pathological alpha-synuclein propagation and autonomic dysfunction in wild-type rats, Brain (2021).
[24] N. Ferreira, N.P. Gonçalves, A. Jan, N.M. Jensen, A. van der Laan, S. Mohseni, C. B. Vægter, P.H. Jensen, Trans-synaptic spreading of alpha-synuclein pathology through sensory afferents leads to sensory nerve degeneration and neuropathic pain, Acta neuropathologica communications 9 (1) (2021) 31.
[25] I.C. Brás, T.F. Outeiro, Alpha-synuclein: mechanisms of release and pathology progression in synucleinopathies, Cells 10 (2) (2021).
[26] I. Choi, Y. Zhang, S.P. Seegobin, M. Pruvost, Q. Wang, K. Purtell, B. Zhang, Z. Yue, Microglia clear neuron-released α-synuclein via selective autophagy and prevent neurodegeneration, Nat. Commun. 11 (1) (2020) 1386.
[27] S. George, N.L. Rey, T. Tyson, C. Esquibel, L. Meyerdirk, E. Schulz, S. Pierce, A. R. Burmeister, Z. Madaj, J.A. Steiner, M.L. Escobar Galvis, L. Brundin, P. Brundin, Microglia affect α-synuclein cell-to-cell transfer in a mouse model of Parkinson's disease, Mol. Neurodegener. 14 (1) (2019) 34.
[28] V. Refolo, N. Stefanova, Neuroinflammation and glial phenotypic changes in alpha-synucleinopathies, Front. Cell. Neurosci. 13 (2019) 263.
[29] M. Bu, M.J. Farrer, H. Khoshbouei, Dynamic control of the dopamine transporter in neurotransmission and homeostasis, NPJ Parkinson's disease 7 (1) (2021) 22.
[30] C.D. Hughes, M.L. Choi, M. Ryten, L. Hopkins, A. Drews, J.A. Botía, M. Iljina, M. Rodrigues, S.A. Gagliano, S. Gandhi, C. Bryant, D. Klenerman, Picomolar concentrations of oligomeric alpha-synuclein sensitizes TLR4 to play an initiating role in Parkinson's disease pathogenesis, Acta Neuropathol. 137 (1) (2019) 103–120.